16A.6 **CLIMATOLOGY OF STORM REPORTS RELATIVE TO UPPER-LEVEL JET STREAKS**

Adam J. Clark*, Christopher J. Schaffer, William A. Gallus, Jr., and Kaj Johnson-O'mara

Iowa State University, Ames, IA.

1. INTRODUCTION

According to the conceptual "four quadrant" model (4QM hereafter; e.g., Bluestein 1993; Rose et al. 2004) for linear upper level jet streak circulations, ageostrophic flow and mass conservation result in upward (downward) motion in the right entrance and left exit (left entrance and right exit) regions of a jet streak. Modifications to the 4QM are required in the presence of curved flow which results in a two-cell, rather than four-cell, pattern of divergent/convergent centers (e.g. Beebe and Bates 1955; Moore and VanKnowe 1992), and further modifications are required in the presence of thermal advection (Shapiro 1983), which can cause jet-induced circulations to be laterally displaced toward either side of the jet axis (e.g., Pyle et al. 2004).

The 4QM is often used as a severe weather forecasting tool, which motivated Rose et al.'s (2004) 10-yr climatological study of F1 and above tornado occurrences relative to 250-hPa jet streak quadrants without considering all the complexities of jet streak dynamics. This study extends the results of Rose et al. (2004) by analyzing the climatology of hail and wind reports, as well as tornado reports, relative to linear and curved upper level jet streaks, as well as examining temporal trends in storm report frequency and sensitivity to jet streak direction. Composite fields (e.g. upper level divergence) are also examined to determine whether these fields match what would be expected based on conceptual models for linear and curved jet streaks.

2. DATA AND METHODOLOGY

The North American Regional Reanalysis (NARR; Mesinger et al. 2006) dataset was used to analyze upper level jet streaks and associated fields. Storm reports (hail, wind, and tornado) as compiled by the Storm Data publication, were obtained from the SPC website (http://www.spc.noaa.gov/climo/historical.html). Bias and quality problems inherent in this database are discussed in Gallus et al. (2008) and references therein. The time period March-September of 1994-2004 was analyzed, and only jet streaks occurring at 0000 UTC that had associated storm reports valid +/- 3-hrs from 0000 UTC were considered, following Rose et al. (2004). Storm reports occurring within this 6-hr time window, but not associated with any jet streak were classified as "non-jet related".

The criterion for jet streak classification was an enclosed area of wind speeds exceeding 25 ms^{-1}. An interactive Grid Analysis and Display System (GrADS) script was used to manually define jet streak regions. For each jet streak that appeared to contain storm reports in any of its quadrants, the user marked the location of the jet core and jet endpoints, as well as the orientation of the minor axis that went through the jet core and jet endpoints and extended 1000-km in both directions perpendicular to the major jet axis. The jet core was defined as a point within the area of maximum wind speed where the acceleration became zero, while the jet ends were defined by following streamlines nearest to the jet core downstream (upstream) through the exit (entrance) region until the acceleration became zero. In addition, the GrADS script required the user to mark a sequence of points following the streamline nearest to the jet core within the exit and entrance region defining the extension of the major jet axis. After each jet was defined, it was divided into a 77x37 grid, with the jet core used as the center gridpoint and the points along the major jet axis with maximum (minimum) acceleration in the entrance (exit) region used as the center gridpoint in the entrance (exit) region. An example of a case that was analyzed for 1 June 1995 is

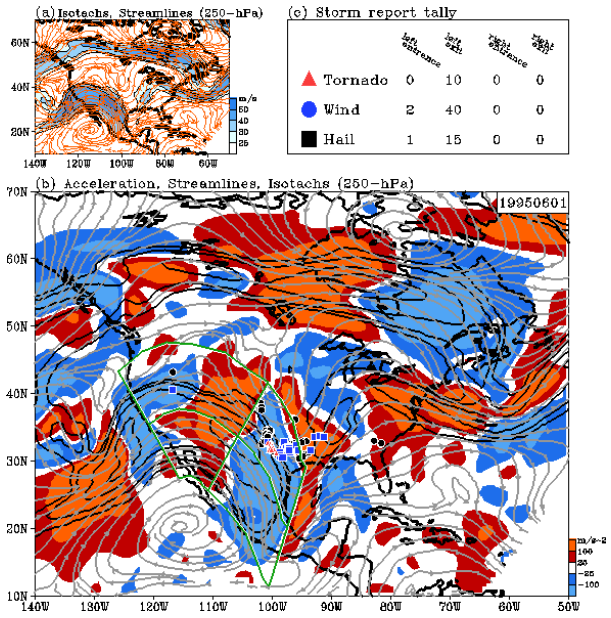

Figure 1 Example of the GrADS interface used to define jet streaks. a) 250-hPa Streamlines and isotachs (shaded), b) 250-hPa acceleration (shaded), streamlines, storm reports (circles, squares, and triangles) and isotachs (black contours), and c) number of each type of storm report in each jet quadrant.

* *Corresponding author address:* Adam J. Clark, Iowa State Univ., Dept. of Geol. and Atm. Sciences, Ames, IA; email: clar0614@iastate.edu.

Table 1 Summary of monthly and total storm report statistics. The first four columns indicate the number (in parentheses) and percentage of jet-related reports occurring in each jet quadrant. The bold values indicate the quadrant with the highest percentage of reports, and the light gray values indicate quadrants with the lowest percentage of reports. The "Unclassified" column shows numbers and percentages of total storm reports (jet- and non-jet-related) not associated with a jet streak. The "Repeats" column shows the number and percentage of the total jet-related storm reports that were associated with more than one jet streak, and the "Total" column is simply the total number of each type of storm report (jet- and non-jet related) that occurred during each month.

MAR	*Left-Entr*	*Left-Exit*	*Right-Entr*	*Right-Exit*	*Unclassified*	*Repeats*	*Total*
Torn	(79) 24.2%	(92) **28.1%**	(92) **28.1%**	(64) 19.6%	(19) 5.5%	(21) 6.1%	345
Hail	(616) 17.5%	(1487) **42.4%**	(792) 22.6%	(615) 17.5%	(41) 1.2%	(402) 11.4%	3536
Wind	(174) 10.9%	(468) 29.4%	(379) 23.8%	(569) **35.8%**	(175) 10.0%	(109) 6.2%	1756
APR							
Torn	(70) 8.8%	(326) **40.9%**	(188) 23.6%	(213) 26.7%	(80) 9.4%	(109) 12.8%	852
Hail	(1233) 12.7%	(3179) **32.8%**	(2604) 26.9%	(2662) 27.5%	(472) 4.8%	(1355) 13.9%	9732
Wind	(384) 10.1%	(1156) 30.3%	(1226) **32.1%**	(1049) 27.5%	(208) 5.3%	(419) 10.7%	3919
MAY							
Torn	(286) 13.7%	(630) **30.1%**	(584) 27.9%	(592) 28.3%	(78) 3.9%	(344) 17.1%	2012
Hail	(2594) 14.5%	(4563) 25.4%	(5934) **33.1%**	(4852) 27.0%	(1187) 6.7%	(2924) 16.5%	17688
Wind	(931) 9.7%	(1632) 17.0%	(4476) **46.5%**	(2577) 26.8%	(1212) 12.1%	(1381) 13.8%	10017
JUN							
Torn	(113) 7.3%	(438) 28.3%	(475) 30.7%	(521) **33.7%**	(58) 3.7%	(212) 13.7%	1547
Hail	(1814) 14.0%	(2843) 21.9%	(4576) **35.3%**	(3740) 28.8%	(1720) 12.2%	(1701) 12.0%	14148
Wind	(1138) 9.7%	(2176) 18.6%	(5622) **48.2%**	(2737) 23.4%	(3057) 21.6%	(1462) 10.3%	14179
JUL							
Torn	(71) 10.0%	(116) 16.3%	(257) 36.1%	(268) **37.6%**	(253) 26.7%	(60) 6.3%	948
Hail	(1205) 16.4%	(1202) 16.4%	(2521) **34.4%**	(2401) 32.8%	(2660) 27.5%	(708) 7.3%	9657
Wind	(741) 7.6%	(973) 10.0%	(4727) **48.7%**	(3258) 33.6%	(4758) 33.4%	(562) 4.0%	14225
AUG							
Torn	(56) 17.6%	(61) 19.2%	(107) **33.6%**	(94) 29.6%	(152) 33.0%	(35) 7.6%	461
Hail	(1021) 18.1%	(1048) 18.6%	(1948) **34.6%**	(1615) 28.7%	(1473) 21.8%	(860) 12.7%	6749
Wind	(710) 10.6%	(726) 10.8%	(3444) **51.4%**	(1814 27.1%	(2949) 31.8%	(716) 7.7%	9285
SEP							
Torn	(29) 12.4%	(30) 12.9%	(122) **52.4%**	(52) 22.3%	(62) 21.5%	(25) 8.7%	289
Hail	(737) 24.9%	(616) 20.8%	(935) **31.6%**	(675) 22.8%	(30) 1.1%	(672) 24.4%	2750
Wind	(448) 15.9%	(465) 16.5%	(1175) **41.7%**	(728) 25.9%	(233) 8.4%	(595) 21.5%	2769
ALL							
Torn	(704) 11.7%	(1693) 28.1%	(1825) **30.3%**	(1804) 29.9%	(702) 10.9%	(806) 12.5%	6454
Hail	(9220) 15.4%	(14938) 24.9%	(19310) **32.2%**	(16560) 27.6%	(7583) 11.8%	(8622) 13.4%	64260
Wind	(4526) 9.9%	(7596) 16.5%	(21049) **45.9%**	(12732) 27.7%	(12592) 22.4%	(5244) 9.3%	56150

provided in Figure 1.

It should be noted that the composite fields, in particular upper-level divergence, could be affected by convection present at the time of the jet streak analysis. An attempt was made to quantify the influence of ongoing convection by comparing composite upper-level divergence for cases in which storm reports did not occur until after 0000 UTC, to cases in which reports occurred before and after 0000 UTC (not shown). These two composites were very similar; thus, no further attempts were made to account for the influence of convection on composite fields.

3. RESULTS

3.1 Jet Streak Climatology and Composite Storm Report Distributions

A total of 3179 jet streaks containing 105,987 storm reports were analyzed, accounting for 84% of the total (126,864) number of storm reports that occurred during the 11-yr period. A full summary of monthly and total storm report statistics is provided in Table 1.

In general, the monthly distribution of jet cores associated with storm reports follows the seasonal northward migration of the jet stream (Figs. 2a-g). The peak month for storm reports, including jet and non-jet related reports, is June, with May having only slightly less reports than June (Fig. 2h; Table 1). During the warm season (June – August), the percentage of jet-related storm reports (top-right panels of Figs. 2a-g) decreases, so that May is the peak month for jet-related storm reports, with June having the second most jet-related reports. A number of factors likely contribute to the decrease in jet-related reports during the warm season. First, strong heating and high humidity often result in high values of CAPE favorable for severe weather despite the presence of weak vertical wind shear in areas far removed from jet streaks. Second, as the North American Monsoon (NAM; Higgins et al. 1997) becomes established and the jet-stream shifts northward, jet streaks occur more often at latitudes north of the US, decreasing the area evaluated in the

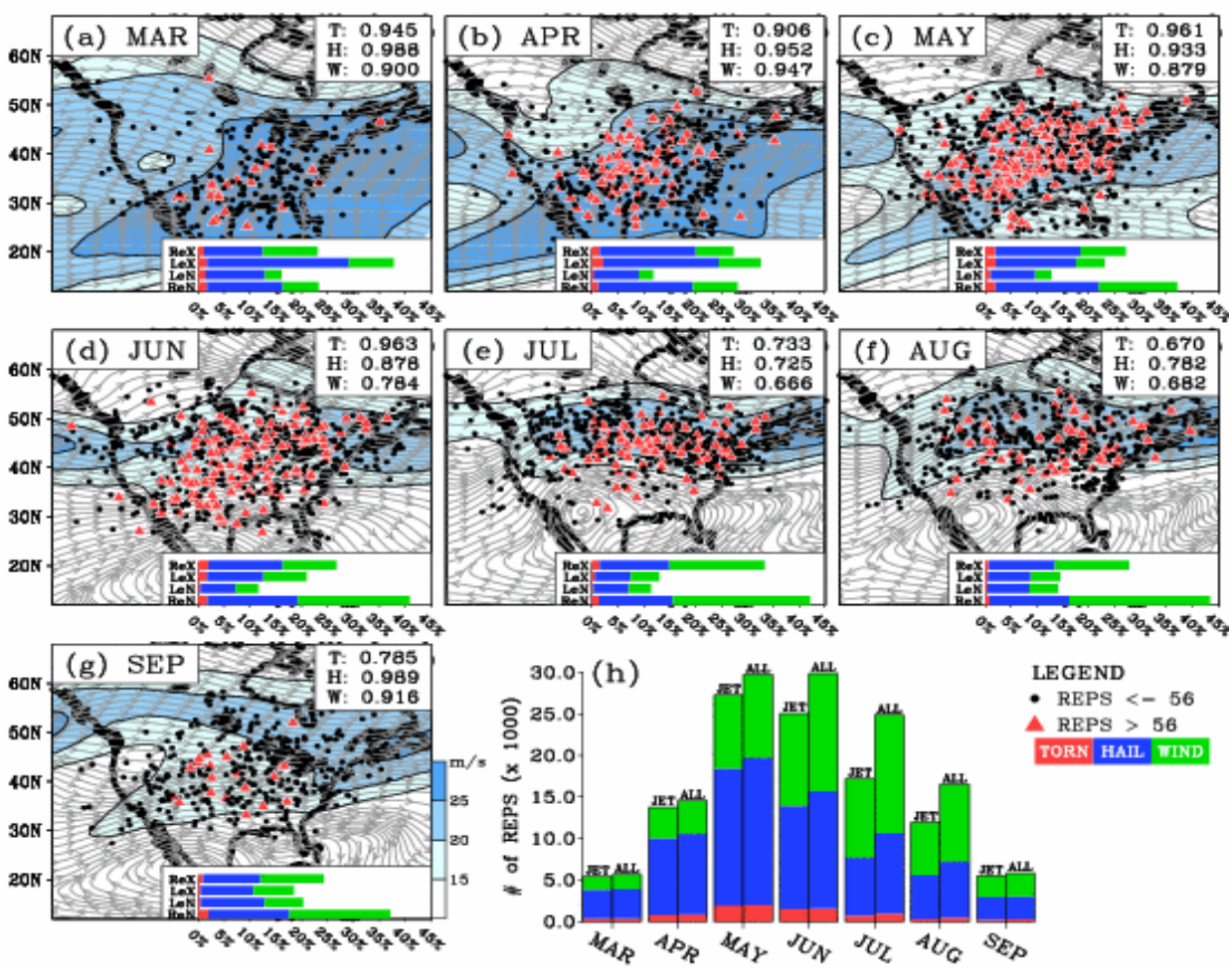

Figure 2 a)-g) Monthly distributions of jet streaks superimposed with monthly average 250-hPa wind magnitude (shaded) and streamlines. Closed black dots (triangles) denote jet streaks associated with less than or equal to (greater than) 56 storm reports (the 80% quantile of jet streak event associated storm report frequency). The values in the top-right corner are percentages of total tornado (T), hail (H), and wind (W) reports associated with jet streaks. The histograms in the bottom-right corner indicate the percentages of tornado (black), hail (light gray), and wind (medium gray) reports in each jet-quadrant (ReX=right exit; LeX=left exit; LeN=left entrance; ReN=right entrance). h) Monthly histogram of jet-related (JET) and total (ALL) storm report frequency.

contiguous US so that jet-related reports decrease, while non-jet related reports may increase or remain relatively constant. Finally, when the large upper-level anticyclone associated with the NAM is established during the warm-season, mid-tropospheric perturbations (MPs; Wang et al. 2008) that are restricted to below 250-hPa, often provide forcing to initiate and sustain long-lived severe weather episodes. These episodes are often associated with progressive MCSs or derechos that area characterized by long swaths of damaging wind reports.

During March and April the majority of storm reports occur in the left-exit quadrant, while after April most reports occur in the right-entrance quadrant (bottom-right portion of Figs. 2a-f; Table 1). Thus, the quadrant containing the most reports is always one of the quadrants favored for upward motion according to the 4QM. If the different types of storm reports are considered separately, there are a few instances when the majority of reports occur in a quadrant not favored for upward motion. For example, the right-exit region is favored for wind reports during March and tornado reports during June and July.

Considering the distribution of reports over all four jet streak quadrants, only March and April have distributions that would be consistent with the circulations predicted by the 4QM. After April, the right-exit quadrant (not favored for upward motion by the 4QM) always contains more reports than the left-exit quadrant (favored for upward motion), and is the quadrant with the second largest number of reports. If only the entrance quadrants are considered, all months have a storm report distribution matching that predicted by the 4QM (Figs. 2a-f).

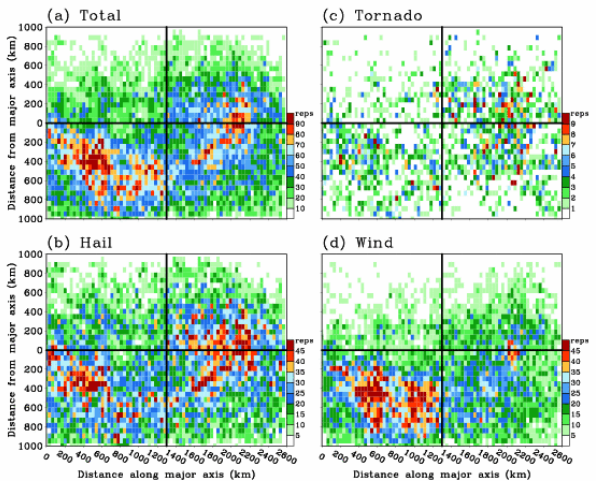

Figure 3 Composite storm report frequencies within a jet streak for a) all reports, b) hail, c) tornadoes, and d) wind. Black lines define the jet streak quadrants.

Composite storm report distributions (Figs. 3a-d) show that storm reports are concentrated in a region along the major jet axis in the exit region east of the point with maximum deceleration, and in another region roughly centered over the right entrance quadrant. Tornado reports appear to be more concentrated in the exit quadrant region, while hail reports are relatively evenly distributed between the two regions, and wind reports are more concentrated in the right-entrance region.

3.2 *Jet Streak Composite Fields*

Composite 250 hPa divergence (Fig. 4a) generally matches what would be expected from the 4QM, and the jet-transverse vertical circulation in the entrance region (Fig. 4e) is stronger than that in the exit region (Fig. 4f). The jet-transverse vertical circulation in the entrance region (Fig. 4e) also generally matches what would be expected from the 4QM, with upward (downward) motion occurring over most of the troposphere in the right-entrance (left-entrance) region and maxima/minima vertical velocities around 400 hPa. The jet-transverse vertical circulation in the exit region (Fig. 4f) only matches the 4QM in the left-exit region where upward motion occurs over the depth of the troposphere. In the right-exit region, only a small area between about 600 and 300 hPa and near the major jet-axis experiences the downward motion expected from the 4QM, while upward motion occurs in much of the lower to mid-troposphere.

Composite mean-sea-level-pressure (mslp; Fig. 4b) reveals a closed surface low centered in the left-exit quadrant, and a trough of low pressure extending from this surface low into the right-entrance quadrant implies the average location of surface fronts. The distribution of storm reports (Figs 3a-d) coincides with what would be expected from the composite upper-level divergence

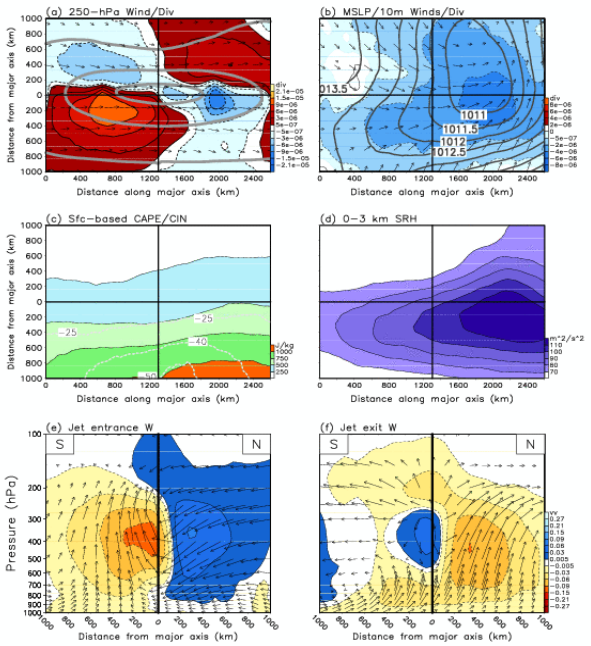

Figure 4 Jet streak composites of a) 250 hPa isotachs (gray contours for 15, 30, and 45 m/s), divergence (shaded), and wind vectors, b) mean-sea-level-pressure, 10-m wind vectors, and 10-m divergence (shaded), c) surface based CAPE (shaded) and CIN (dashed contours), and d) 0-3 km SRH. Jet-transverse cross sections of vertical velocity (Pa/s; shaded), and circulation vectors composed of the vertical component and v-component of the flow for the e) entrance, and f) exit regions.

fields (Fig. 4a) only if the entrance regions are considered. In the exit region, the area of strongest upper-level divergence is north of the area with the most storm reports, and the maximum in storm reports located along the major jet-axis occurs in the presence of upper-level convergence. The exit region storm reports appear to coincide much more closely with low-level convergence than with upper-level divergence.

In addition to support from low-level convergence, the high relative frequency of storm reports in the right-exit region is also explained by composites of basic severe weather parameters which show that convective available potential energy (CAPE; Fig. 4c) tends to be highest in the right-exit region, as well as 0-3 km storm relative helicity (SRH; Fig. 4d). Thus, although the jet-induced vertical circulation is not conducive to severe weather in the right-exit region, other processes counteract the jet streak processes making storm reports in this region very common, which was also discussed by Rose et al. (2004).

3.3 Effects of Jet Curvature

A procedure was devised to estimate the radius of curvature for the jet streaks analyzed in this study to

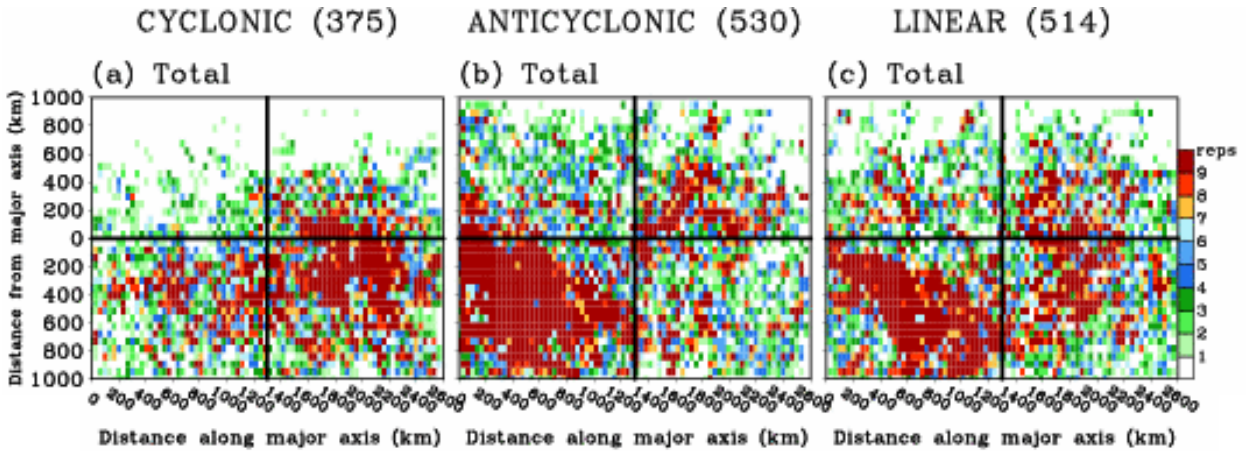

Figure 5 Distribution of total storm report frequencies associated with a) cyclonic, b) anticyclonic, and c) linear jet streaks.

examine the effects of jet streak curvature. The changein jet streak direction (Δd; in radians) along the major jet axis was calculated using the mid-points of the exit and entrance regions, and the distance between these two mid-points, L, along the major jet-axis was computed. Using the formula for the circumference of a circle, $C=2\pi R$, it is easily shown by substituting $(2\pi/\Delta d)*L$ for C, that $R=L/\Delta d$, which estimates the radius of curvature. Note that this estimate is for the radius of curvature of streamlines, not trajectories, so that large errors could be introduced during computation of fields dependent on R, like centripetal acceleration (Holton 2004). However, for the purposes of this study, this estimate should be adequate.

The distribution of jet curvatures (not shown) is slightly weighted towards jet streaks with anticyclonic curvature. Jet streaks with $R \leq 2{,}000$ km are classified as cyclonically curved, those with $R \geq -2{,}000$ km are classified as anticyclonically curved, and those with $R \geq 10{,}000$ km or $R \leq -10{,}000$ are classified as linear. Storm reports are all more frequent in the exit quadrants of cyclonically curved jet streaks than the entrance quadrants (Figs. 5a, d, g, and j), with maxima centered approximately along the major jet-axis, while the opposite is apparent for anticyclonically curved jets (Figs. 5b, e, h, and k), with maxima within the right-entrance region.

Composite 250 hPa divergence for each class of R (Figs. 6a-c) generally matches what would be expected from conceptual and numerical models. For anticyclonically curved jet streaks (Fig. 6b) the divergence and convergence maxima are stronger than for cyclonically curved jet streaks, with the divergence (convergence) maxima in the right-entrance (right-exit) quadrant. Jet-transverse cross sections also show stronger vertical velocity in anticyclonic jet streaks than in cyclonic jet streaks. For linear jet streaks the familiar four cell pattern of divergent/convergent centers is apparent (Fig. 6c). The strongest vertical velocities in linear jet streaks, which occur in the left-exit quadrant (Fig. 6f), are weaker than the strongest vertical velocities that occur in the left-exit quadrant of

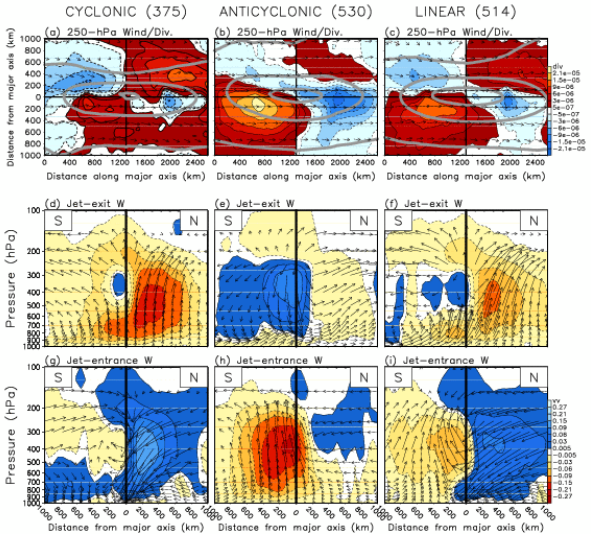

Figure 6 a) – c) same as 4a, except for a) cyclonic, b) anticyclonic, and c) linear jet streaks. d) – f) same as 4f, except for d) cyclonic, e) anticyclonic, and f) linear jet streaks. g) – i) same as 4e, except for g) cyclonic, h) anticyclonic, and i) linear jet streaks.

cyclonically curved jet streaks (Fig. 6d), and weaker than those that occur in the right-entrance region of anticyclonically curved jet streaks (Fig. 6h).

For cyclonically curved jet streaks (Fig. 7a), a closed center of low-pressure is centered along the major jet-axis in the center of the exit region. An area of strong relative convergence coincides with this surface low, as well as a maximum in storm report frequency (Figs. 5a, d, g, and j). Also, note that the area where relatively strong low-level convergence occurs also tends to have low-level wind shear (Fig. 7g) and convective instability (Fig. 7d) sufficient for severe storms.

For anticyclonically curved jet streaks (Fig. 7b), an area of surface low-pressure exists in the right-entrance quadrant. Similar to the cyclonic jet streaks, an area of

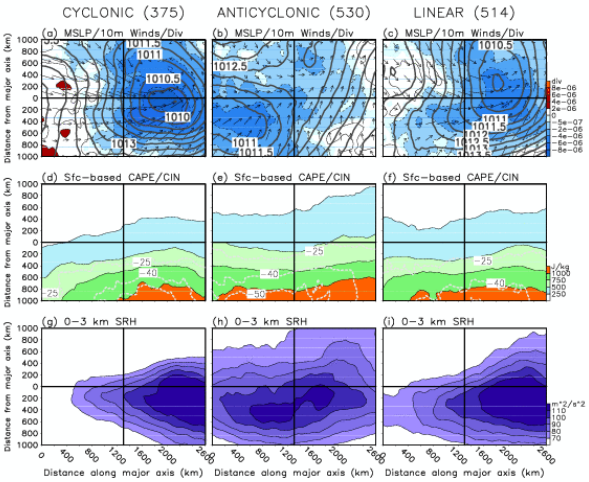

Figure 7 a) – c) same as 4b, except for a) cyclonic, b) anticyclonic, and c) linear jet streaks. d) – f) same as 4c, except for d) cyclonic, e) anticyclonic, and g) linear jet streaks. g) – i) same as 4d, except for g) cyclonic, h) anticyclonic, and i) linear jet streaks.

strong relative convergence coincides with this area of low-pressure, except it is not as strong as in the cyclonic jet streak composite. Also similar to the cyclonic jet streak composites, the storm report distributions for anticyclonic jet streaks correspond very closely to the area of relatively strong low-level convergence in the anticyclonic jet streak composite. In general, combinations of favorable shear and instability for severe storms cover the largest area in anticyclonic jet streaks. However, the coverage of severe reports (Fig. 6) is similar to that in linear jet streaks, which have a larger region favored for severe weather by upward motion as inferred from the jet-transverse cross sections of vertical velocity (Figs. 6d-i).

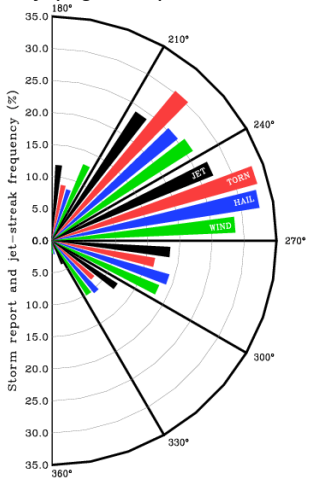

Figure 8 Percentage of jet streaks (black) within the range of directions indicated by the portions within the half circle, and percentage of tornado (light-gray), hail (dark-gray), and wind (medium-gray) reports associated with jet streaks within each specified range.

3.4 Effects of Jet Directions

To examine what impact the direction of the jet streak may have on severe weather reports, jet streaks are categorized into six ranges of directions: SSW (180-210°), SW (210-240°), WSW (240-270°), WNW (270-300°), NW (300-330°), and NNW (330-360°). 98% of the jet streaks analyzed fell within these ranges. The remaining 2% of jet streaks, which had directions with easterly components, were not analyzed because they represented such a small sample of cases.

WSW jet streaks were most frequent (27.1%), closely followed by SW jet streaks (24.0%), and then WNW (18.5%), NW (12.3%), SSW (11.8%), and NNW jet streaks (4%; Fig. 8). Generally, the ranking of percentages of storm reports associated with each jet streak direction followed the ranking of jet streak percentages, but the SW and WSW directions were especially active with the percentage of storm reports higher than the percentage of jet streaks (Fig. 8).

Composites for different jet streak directions revealed SSW jet streaks were associated with the strongest upward vertical velocities, and there was a trend for decreasing upward vertical velocities as jet streak directions rotated clockwise (Fig. 10). The majority of storm reports were associated with SW and WSW jet streaks (Fig. 9), which were associated with modest jet-induced upward vertical velocities and an ideal configuration of low-level winds and instability for severe weather (not shown).

4. Conclusions

Identifying favorable regions for the development of severe weather is a challenging aspect of operational forecasting, and many different fields/parameters must be considered when generating severe weather forecasts. Consideration of the 4QM and the position of upper-level jet streaks relative to low-level features is helpful when determining risk areas, and the results from this study should provide additional insight to forecasters when considering the influence of upper-level jet streaks on severe weather potential.

5. Acknowledgments

This research began as part of a required senior meteorology undergraduate thesis course at Iowa State University taught by Eugene Takle. This research was also supported by NSF Grant ATM-0537043, and useful discussions with Shih-Yu (Simon) Wang regarding mid-tropospheric perturbations were much appreciated.

6. References

Available upon request.

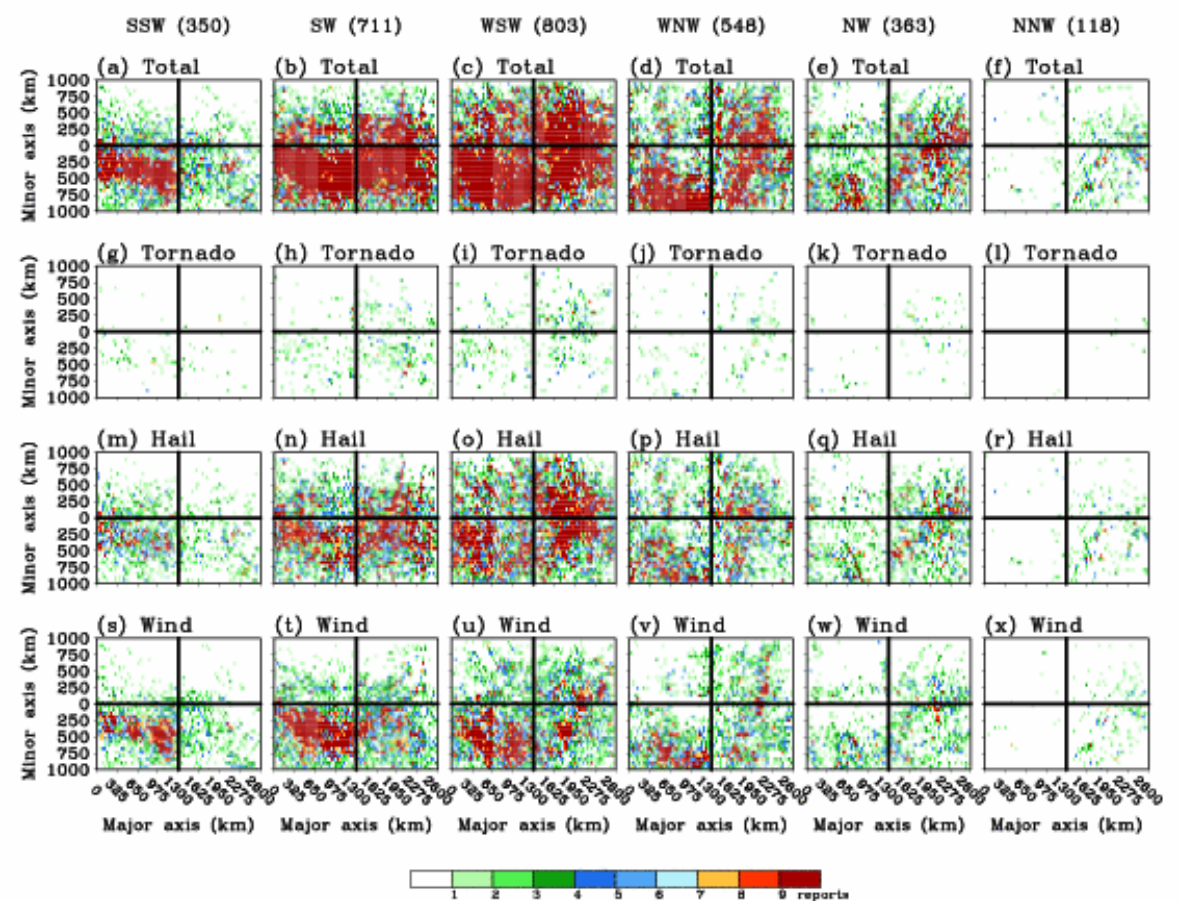

Figure 9 Distribution of total storm report frequencies for a) SSW, b) SW, c) WSW, d) WNW, e) NW, and f) NNW jet streak directions. g) – l), m) – r), and s) – x) same as a) – f) except for tornado, hail, and wind reports, respectively.

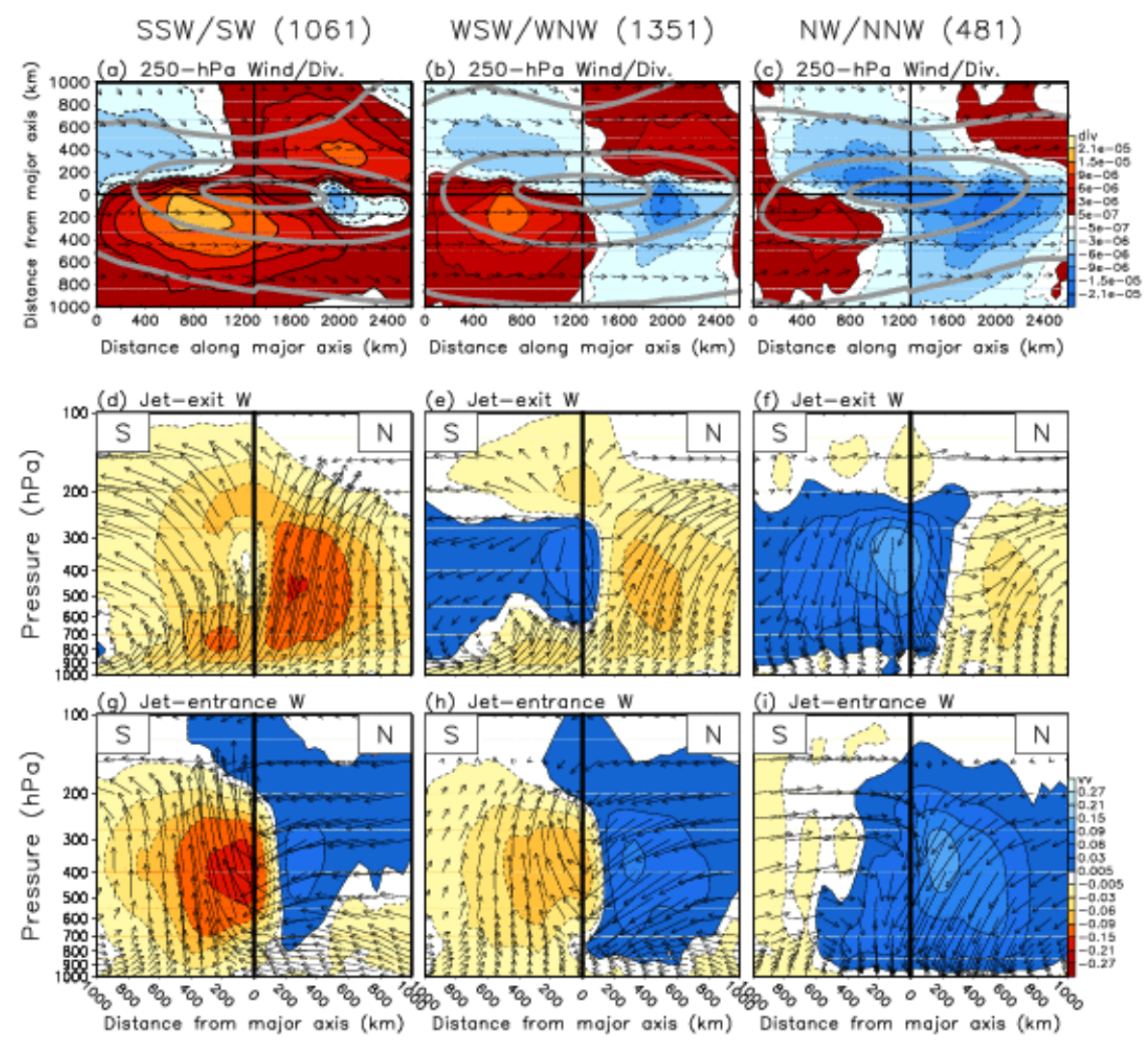

Figure 10 Same as Fig. 6, except for SSW/SW, WSW/WNW, and NW/NNW jet streak directions.